Challenge Journal of Structural Mechanics

Research Article

An insight into design of prefabricated and prestressed concrete monoblock railway ties for service loads

Niyazi Özgür Bezgin *

Department of Civil Engineering, İstanbul University-Cerrahpaşa, 34320 İstanbul, Turkey

ABSTRACT

Ballasted railway track ties support the wheel forces of a train that are transferred onto them by the rails, maintain the track gauge and provide lateral and longitudinal track stability. Prestressed concrete ties provide the required track bearing to the applied wheel loads and constitute a major part of the track self-weight. Design of prestressed concrete ties involves an evaluation of their structural interaction with the ballast and an understanding of prestressed concrete design for service loads and beyond-service loads. This paper aims to provide an insight for the design of a prestressed concrete ballasted railway tie under service loads and highlight the genuine qualities of tie design in terms geotechnical engineering, materials engineering and structural engineering. Through the analysis of a finite element model, this paper presents estimations for bending moment values under service conditions for a prestressed concrete high-speed railway tie under varying track support conditions. The paper then compares the estimated values with those suggested by the relevant design guidelines for railway ties.

ARTICLE INFO

Article history:
Received 1 June 2018
Revised 8 September 2018
Accepted 25 September 2018

Keywords:
High-speed railways
Prefabrication
Prestressing
Monoblock railway ties
Finite element method
Soil-structure interaction
Service load design

1. Introduction

Modern guided ways for trains provide service through ballasted railway tracks, railway slab tracks, monorails and more recently, the maglev tracks and the hyperloop. The first three types of tracks rely on the adhesion between track rail and train wheel for motion whereas the maglev relies on the magnetic field between the levitating electrified trains over the electrified track exposed to open air. The hyperloop also relies on magnetic levitation where the guided motion takes place in a vacuumed tube. However, maglev tracks are yet to achieve design maturity and economic viability whereas the hyperloop is in early stages of research and development. Albeit their higher initial construction costs compared to ballasted tracks, increasing uses of slab-track railways through tunnels, over the bridges and along railway routes with frequent high-speed railway service, provide weight and structural gauge reduction and reduced maintenance costs (Lichtberger, 2011).

Ballasted railway tracks with monoblock concrete ties, which are the highlight of this paper, currently provide an economical and a reliable solution to most railway transportation needs today. Fig. 1 that is modified by the author to show the sloping subballast layer for drainage, shows a common cross-section of a single ballasted track on a fill (Ebrahimi et al., 2011). Ballasted railway track superstructure consists of rails, elastomeric bearing pads underneath the rails, attachment and bearing elements for rails to ties, the ties that support the rails via bearing on ballast layer, the ballast layer and subballast layer The platform grade achieved by the fill or reached and prepared by the cut constitutes the substructure or the subgrade under which lies the natural or existing ground.

The tie shown in Fig. 1 is a monoblock type of tie. The elastomeric bearing pads between the rails and the concrete tie reduce the bearing stiffness of the steel rails on the concrete tie and reduce the dynamic impact force on the tie depending on their attenuation characteristics. Ties interact with the supporting ballast layer through bearing and bending under vertical loads and shear under lateral loads.

The ballast and the sub-ballast layers consist of aggregates that reduce the bearing pressures exerted by the tie

* *Corresponding author*. Tel.: +90-212-4737070 ; E-mail address: ozgur.bezgin@istanbul.edu.tr (N. Ö. Bezgin)
ISSN: 2149-8024 / DOI: https://doi.org/10.20528/cjsmec.2018.04.001

to pressure values allowed on the subgrade. The sub-ballast has the primary duties of providing drainage and filtering for the ballast layer above and frost protection for the subgrade below in addition to their added benefit for reducing bearing pressures on the subgrade (Navikas et al., 2016).

Contemporary railway tracks have performance requirements with respect to service speeds and service loads. International Union of Railways (UIC) recommends track design values for member and affiliated states. Table 1 presents the static design axle loads and train speeds for modern railway tracks (UIC-713R, 2004).

This study concentrates on the evaluation of the design bending moments for the tie under ordinary service load conditions. A finite element model developed for the analysis of the tie under the pseudo-dynamic action of the service loads provides an estimate for the required design bending moments under service loads and the prestressing force required to maintain the stress values at acceptable levels under the service load condition. The study provides a comparison of the UIC service design recommendations with the estimates obtained from the finite element analysis.

Table 1. Combined axle forces and train speeds.

	Static axle force (kN)		
Speed (km/h)	180	225	250
120	♦	♦	♦
200	♦	♦	None
300	♦	None	None

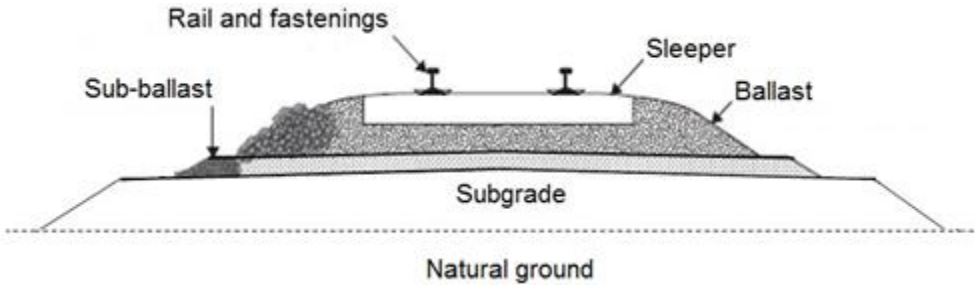

Fig. 1. Cross-section of a single ballasted track on a fill (Modified from Ebrahimi et al., 2011).

2. Prestressed Concrete Ties

Following their introduction in 1950's, many countries developed their unique geometric designs of prefabricated high performance concrete ties. For instance in Germany, concrete ties has unique notations such as B58, B70, B90 and B07 where the letter B denotes the word "beton" and the last two digits signifies the last two digits of their year of introduction (Kerr, 2003). A prestressed monoblock tie shown in Fig. 2 has a length of 2600 mm and an approximate mass of 290 kg. C60 grade concrete and an initial prestressing load of 350 kN under very low design humidity conditions that result in 30% prestress losses, provide the sufficient strength and stiffness for the stresses that occur under a design axle force of 225 kN and a design speed of 250 km/hour.

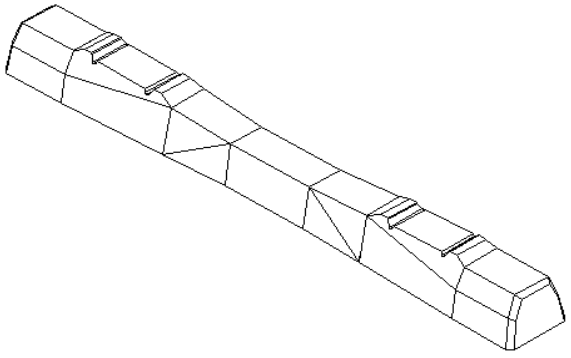

Fig. 2. Perspective view of a prestressed monoblock tie.

Along with bending moment strengths of the tie at the rail seat section and the central section, the ties must have sufficient mass to provide lateral track stability against track buckling and lateral axle loads at curvatures. The tie mass is approximately 2.5 times higher than a creosote infused pinewood tie. The self-weight of the track and the embedment within the ballast layer provides lateral resistance against buckling and lateral forces. A heavier track provides a more stable guide-way for high-speed travel and improves the lateral resistance against track buckling (Kish and Samawedam, 1991).

3. Estimation of Design Moment Values through Finite Element Analysis

Analysis and design of a prestressed concrete tie under vertical wheel forces requires a soil-structure interaction analysis of an axially prestressed non-prismatic concrete element bearing on a ballast layer under the vertical axle loads of a railway vehicle. The first step in the tie analysis is the determination of the distribution of the wheel forces on the ties by the rails followed by an analysis of the bearing stress distribution along the tie base that influence the magnitude and the variation of the bending moments along the tie. Design of the ties must also take into account environmental issues such as seasonal ambient relative humidity values as they heavily influence the effective prestressing force values that remain in the tie in time (Bezgin, 2015). The following sections highlight these issues in detail.

4. Wheel Load Transfer

Rails transfer the vertical forces from the wheels to the ties. Fig. 3 shows a profile sketch of a ballasted railway on a fill. The wheel positioned on the rail right above a tie does not transfer its full vertical load on the tie directly below but transfers parts of the vertical load to the ties neighbouring the centre tie through the bending stiffness of the rail with respect to the compressive stiffness of the supporting ballasted track.

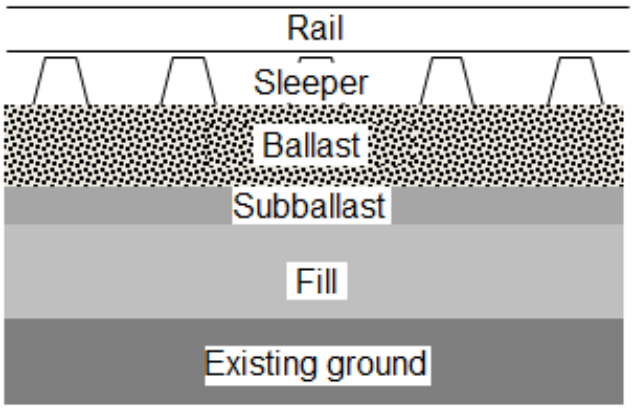

Fig. 3. Profile of a ballasted railway superstructure and substructure on a fill.

For a given combined stiffness of ballast, sub-ballast and subgrade, the transferred amounts of vertical wheel load relates to the bending stiffness (K) of the rail, which directly relates to the bending rigidity of the rail (EI) and inversely relates to the centerline spacing of the ties (L). An increase in the value of L for a given rail rigidity lowers the bending stiffness of the rail, which results in a lower amount of load transfer to neighbouring ties. For a given L and E value, the reduced moment of inertia of a shallower rail also lowers its bending stiffness.

A UIC-60 type rail is 172 mm deep and 150 mm wide at its base. It has a cross-sectional area of 76.7 cm^2, moment of inertia of 3038.3 cm^4 and a mass of 60.2 kg/m (EN 13674, 2002). Existing research indicates that for a UIC-60 type rail supported by ties positioned at 60 cm center-to-center, the wheel loads transfer such that the center-tie that is immediately under the acting wheel receives 50% of the wheel load and the left and right ties neighboring the center tie receive 25% of the wheel loads respectively. Figure 4 shows a two-dimensional linear-elastic model of a UIC-60 rail supported by ties spaced at 60 cm center to center spacing. The static wheel force acting on the rail is 122.5 kN or 12.5 Ton-f, representing the wheel force of a freight train. The coefficient of subgrade reaction (C) for the ballast supporting the ties is 0.3 N/mm^3 representing a newly laid and tamped typical ballasted track.

Fig. 5 shows the developed reactions under the ties in units of kg-f. The tie immediately under the acting wheel load provides a reacting force of 58 kN, which is approximately 48% of the acting wheel force and the neighbouring ties provide about 31 kN reactive force each, which are 26% of the acting wheel force. Therefore, the results of the static analysis of the linear-elastic model presented in Fig. 4 shows that with the given configuration, an estimation of 50% of the wheel load for the heaviest loading on the tie is acceptable.

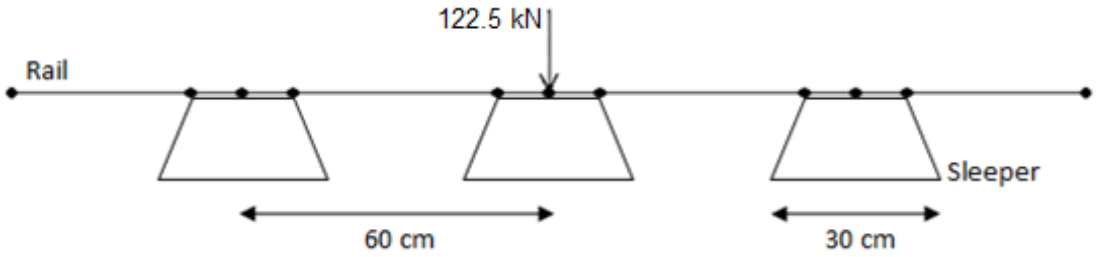

Fig. 4. Two-dimensional load distribution model (ballast support not shown).

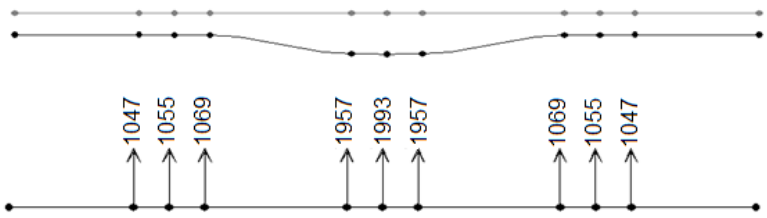

Fig. 5. Reaction distributions under the ties.

One can deduct from the above analysis that wheel load transfer varies by varying tie spacing and/or the section properties of the rail. Theoretically, if the rail had zero bending stiffness, that is to say if the rail was infinitely flexible, the acting wheel load on the rail would completely act onto the tie immediately below. At the other theoretical extreme, if the rail was infinitely stiff compared to the combined stiffness of the track elements below, all three ties in this model would settle the same amount under the acting wheel load and thus each would share one third of the acting wheel load.

5. Bearing Stress and Bending Moment Distribution along the Tie

Upon estimating the transferred maximum value of the wheel load acting on a tie, one needs to investigate the distribution of bearing pressures under the tie and bending moment values along the length of the tie under different bearing conditions. The coefficient of subgrade reaction (C) of a supporting granular medium is a fundamental parameter that influences the amount of settlement in the medium, which occurs under an acting pressure. This coefficient is also an indicator of the compressive stiffness of the granular medium. Based on extensive test data on existing tracks, a properly tamped and stabilized ballast layer of a new track can provide a C value as high as 0.3 N/mm^3 (MPa/mm) (Lichtberger, 2005; Ebrahimi et al., 2015). A weakened ballast layer due to infiltration of thin granular materials, known as fouled ballast can be as low as 0.02 N/mm^3 (MPa/mm) (Ebrahimi et al., 2015). Distribution of bearing pressures and bending moments relates to the compressive stiffness of the ballast layer, the bending stiffness of the prestressed concrete tie and their relative value.

Fig. 6 shows the perspective and top views of finite element model of the tie that is 260 cm long. The width of the tie at its base varies from 30 cm at the ends to 22 cm at the tie centre. The depth of the tie varies from 21.5 cm at the rail seat to 17.5 cm at the tie centre. The meshing includes 45 layers along the length of the tie, 5 layers along the width of the tie and 10 layers along the depth of the tie that amounts to a finite element model with 2250 elements. The model generated by SAP2000® is a linear-elastic model. The tie rests on a ballasted track represented by linear-elastic vertical springs. The bottom view of the tie shows the linear-elastic springs attached to the base nodes of the tie. The solid elements that generate the model are 8-node solid elements. The number of layers along the depth of the tie is selected to prevent the occurrence of the phenomenon known as shear-locking observed in finite element models built with 8-node solid elements.

Design modulus of elasticity (E) for the tie is E=38,000 MPa for a minimum C60 grade concrete produced with hard limestone aggregate. The high strength is necessary in order to provide sufficient early strength for prestressing transfer into the tie. The method of introducing prestressing forces into the tie is using end-bearing plates attached to the prestressing wires by cold-formed buttoning of the wires to the plates. It is important to note that the concrete elastic modulus is very important in prestressed concrete design and varies with the type of aggregate for a given class of concrete. The cross-sectional area along the tie length is variable and the cross section area at the rail seat is A_1 = 555 cm^2 and the cross section area at the tie centre is A_2 = 333 cm^2. Moment of inertia of the tie cross section area is variable along the tie axis of symmetry and varies from I_r = 15,724 cm^4 at the rail seat to I_c = 8,465 cm^4 the tie centre.

Multiple counts of finite element analysis of this tie under 225 kN static axle force distributed by 50% on to the tie by the rails took place over supporting ballast layers with varying coefficient of subgrade reaction values of C = 0.02, 0.05, 0.1, 0.2, 0.3 and 0.4 MPa/mm. The lower bound of these values represents highly fouled ballast bed and the upper bound selected by the author to represent a new ballast bed of granite aggregates with full aggregate interlock. The multiple analyses under the wheel forces transferred by the rails yielded bearing pressure values and bending moment values along the 260 cm length of the tie determined at 26 data points. Figs. 7 and 8 present the respective analyses results for C = 0.02, 0.1, 0.2 and 0.4 MPa/mm.

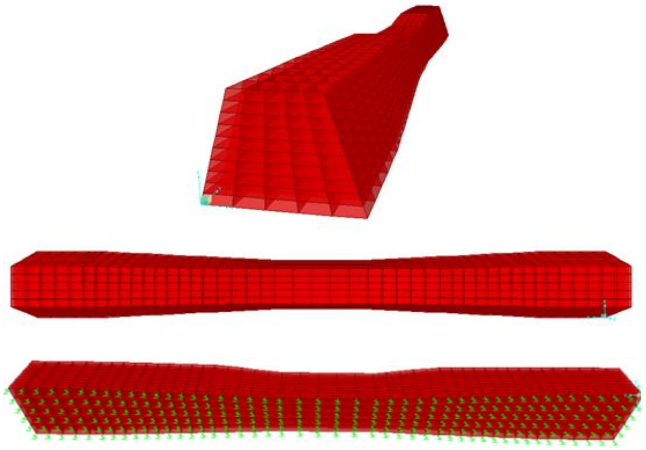

Fig. 6. Perspective views and plan of finite element model of the tie.

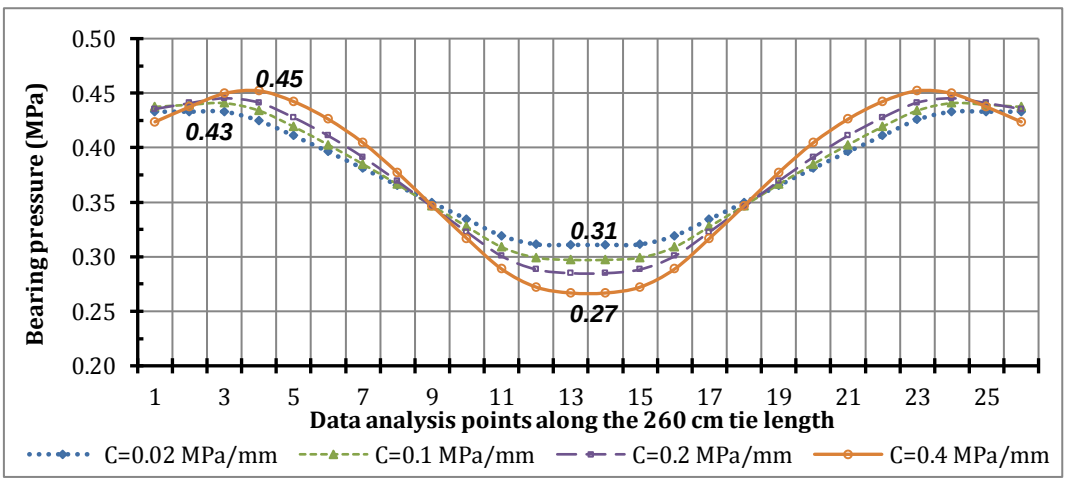

Fig. 7. Pressure variations under ties on ballast layers with varying C values.

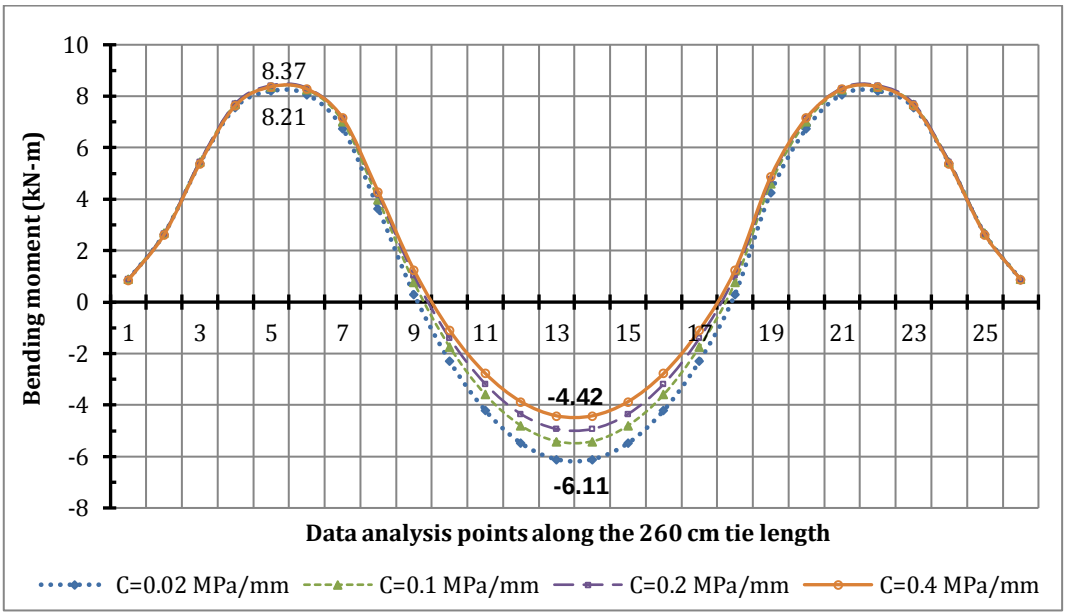

Fig. 8. Bending moments along ties bearing on ballast layers with varying C values.

For a given type of tie, variation of the compressive stiffness of the ballast layer for different coefficient of subgrade reaction values influences the distribution of the ballast bearing pressure and bending moment along the tie. For a given tie bending stiffness, as the compressive stiffness of the supporting layer increases the relative stiffness of the tie with respect to the supporting layer decreases. Therefore, the bearing pressure distribution along the bottom of the tie concentrates and increases along the regions that are under the rails and decreases at the center of the tie. One can think of a theoretical case where the bending stiffness of the tie is negligible and the tie rests on an infinitely rigid ballast layer. Under such conditions, the reactive forces to the acting rail forces on the tie will concentrate right under the rails. However, as the compressive stiffness of the ballast decrease and the relative stiffness ratio of the tie with respect to the ballast increase, the bearing pressures does not concentrate under the rails and increase in the center of the tie and tend to distribute more evenly along the tie. Figs. 7 and 8 clearly show this behavioral tendency for ties under a fixed value of distributed wheel forces supported by ballast layers with varying stiffness values. When the coefficient of subgrade reaction changes from C=0.4 MPa/mm to C=0.02 MPa/mm, the maximum bearing pressure at the middle of the tie increases roughly 13% and maximum bearing pressure at the rail seat regions decrease roughly 4.5%.

Variation of the bending moment also changes with the bearing stress distribution. For the mentioned change of the coefficient of subgrade reaction, the bending moment at the tie center increases roughly 38% whereas the rail seat moments decreases 2%. The effects of the variation of bearing stress values at the tie centre and the rail seats on the bending moment values at the respective locations are not the same due to varying moment of inertia values of the tie cross section area between the rail seat and the tie centre. Fig. 9 shows the variation of the highest rail seat (M_r^+) and tie center (M_c^-) bending moment values along the tie with increasing values of coefficient of subgrade reaction from typical low levels to high levels encountered in practice. With increasing ballast layer stiffness, the tie center moment values reduce profoundly and and the rail seat bending moment values increase slightly.

Previous analytical findings show that for a given tie material and geometry, tie response relates to the stiffness of the supporting granular medium. Determination of stresses due to tie bending under axle loads requires a definition of the support conditions. Table 2 summarizes the findings presented in Fig. 9 and shows the sensitivity of the bending moments at the rail seat and the tie center to coefficient of subgrade reaction of the track. The normalized values are with respective to C=0.02 kN/mm^3 and the related moment values.

One can see with these results that there is a practical limit to track stiffness. Decreased C values increase the bending moment values at the tie centre profoundly and they have a negligible effect on the bending moment values at the rail seat. However, increasing the C values beyond C=0.3 kN/mm^3 does not produce a substantial benefit with respect to the reduction of bending moments at the tie centre.

Within the analysis range for varying coefficient of subgrade values, the underlined highest tie centre moment in Table 2 is M_c^-max=6.11 kN-m which occurs for the low value of C=0.02 MPa/mm. The underlined highest rail seat moment is M_r^+max =8.44 kN-m which occurs for the high value of C=0.4 MPa/mm. Tie design must account for possible variations in the ballast support conditions and must therefore consider the maximum bending moment values that may occur as a result of these variations. The presented analysis results based on the moment envelope indicates a ratio of maximum moments M_r^+max / M_c^-max ~ 1.38 for the tie.

The next section introduces a stress analysis of a tie through a finite element model. The ballast support conditions for the tie is C=0.3 MPa/mm, which is a representative value of a newly constructed and consolidated track.

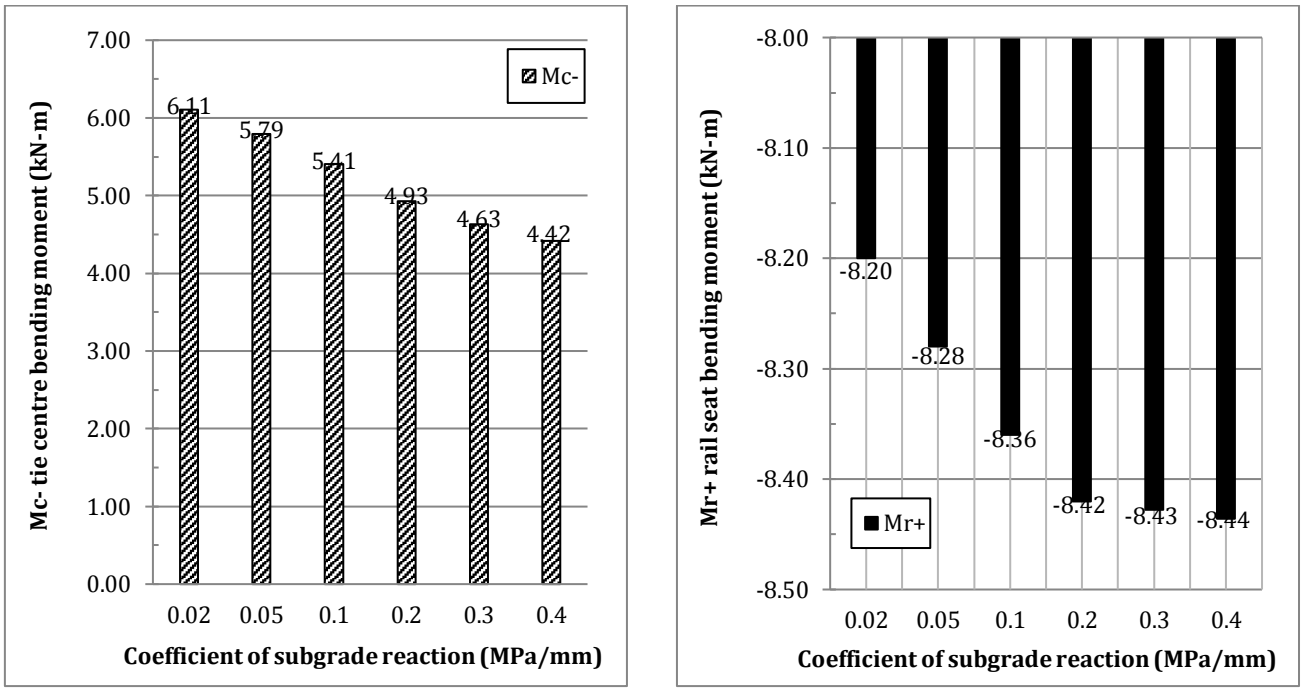

Fig. 9. Variation of maximum rail seat (M_r^+) and tie centre (M_c^-) moment values with C.

Table 2. Tabulation of bending moment values with respect to varying coefficient of subgrade reaction values.

C (kN/mm³)	M_c^- (kN-m)	M_r^+ (kN-m)	$C_{\text{normalized}}$	$M_c^-{}_{\text{normalized}}$	$M_r^+{}_{\text{normalized}}$
0.02	-6.11	+8.20	1.0	1.000	1.000
0.05	-5.79	+8.28	2.5	0.948	1.010
0.1	-5.41	+8.36	5.0	0.885	1.020
0.2	-4.93	+8.42	10.0	0.807	1.027
0.3	-4.63	+8.43	15.0	0.758	1.028
0.4	-4.42	+8.44	20.0	0.723	1.029

6. Stress Analysis of the Tie through a Finite Element Model with respect to Design Conditions

Tie design requires the determination of the location of the prestressing wires in the tie and the value of the prestressing force. The static design axle force on the tie supported over a newly consolidated stiff ballast layer with a design coefficient of subgrade reaction value of C=0.3MPa/mm is Q_{0s}=225 kN.

The static value of the axle force increases due to motion of the train and the unavoidable vertical irregularities along the track caused by the variations in track profile and/or track stiffness. Numerous procedures estimate the possible dynamic impact forces of the moving train wheels on the track and the supporting ties (AREMA, 2006; Bezgin, 2017, 2018). These procedures approach the problem through the interaction of the wheels of a speeding train with the irregularities of the track due to settlements and stiffness variations along the track and with the stiffness and damping properties of the wheel and bogie configuration of the train. All of these procedures may assist the designer to estimate the dynamic axle loads of a moving train on the track. Upon a thorough consideration of the existing approaches, the designer of the presented tie elected to use a conservative dynamic load estimation procedure based on train speed and wheel diameter, which yielded the highest dynamic load estimate. The design speed (v) and wheel diameter (D) of the train is 250 km/h and 920 mm respectively. Eq. (1) empirically presents the dynamic axle load coefficient (ø) based on the estimation by the American Railway and Maintenance Right of Way (AREMA).

$$\emptyset = \left(1 + 5.21\frac{v}{D}\right) = \left(1 + 5.21\frac{250}{920}\right) = 2.4\,. \quad (1)$$

Eq. (2) presents the design service dynamic axle force on the rail supported by the tie:

$$Q_{0d} = Q_{0s} \cdot \emptyset = 225 \cdot 2.4 = 540 \text{ kN}\,. \quad (2)$$

The distributed value of the axle force on the supporting tie is 270 kN, based on a distribution factor of 50% confirmed earlier. Depending on its characteristics, the elastomeric bearing pad between the rail and the tie reduces the transferred dynamic wheel load by the rail onto the tie. The elastomeric bearing pad is an important component of railway superstructure and thus an important

analytical parameter on its own, and therefore the following finite element model excludes the bearing pad to remove a parameter that affects the analysis.

The fundamental design requirement for the tie behaviour under design service loads is to remain uncracked under bending. The finite element model generated by the solid elements and analyzed by the elastic un-cracked analytic capability of the SAP 2000® program determined the bending stresses for the tie under service load conditions. The tensile bending stresses formed the basis for the introduction of the prestressing forces and determination of the prestressing force value. Under the combined action of the 270 kN axle force on the rails, distributed to the tie, tensile stresses occur along the tie bottom underneath the rails and the tie top face at the tie centre. Fig. 10 highlights the tensile bending stresses.

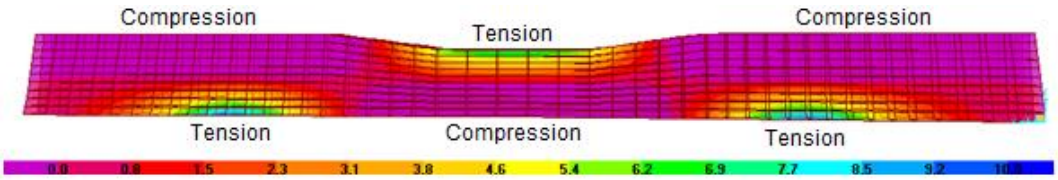

Fig. 10. Tensile and compressive stresses within the tie under 122.5 kN axle force.

Flexural tensile stress values vary from 5 MPa at the top surface of the tie middle to approximately 7 MPa at the tie bottoms under the rail seats, which would crack the C60 grade concrete with a characteristic flexural tensile strength value of 4.3 MPa. Therefore, the prevention or the limitation of these bending stresses is the reason for introducing prestressing forces into the tie.

Fig. 11 conceptually presents the application of the initial prestressing force (P_i) longitudinally into the tie through the center of the force and the longitudinal tie contraction. The tie contracts approximately 0.5 mm under the 350 kN initial prestressing force generating compressive longitudinal stresses along the length of the tie. The compressive stresses vary up to 10 MPa at the tie center, 7 MPa at the rails seats and 12 MPa to 33 MPa at the tie ends. In the particular case, bearing plates anchored into the tie ends introduces the 350 kN prestressing force into the tie generating a bearing stress of approximately 33 MPa. The design and selection process for the anchor plates is the subject of another study. Fig. 12 presents the cross section view of the tie section at the tie ends where the end-bearing plates introduce the prestressing forces into the tie by the BBRV system (plates not shown). BBRV stand for the initials of the last names of the developers “Brandestini, Birkenmaier, Ros and Vogt” who developed the system in the early 1960’s.

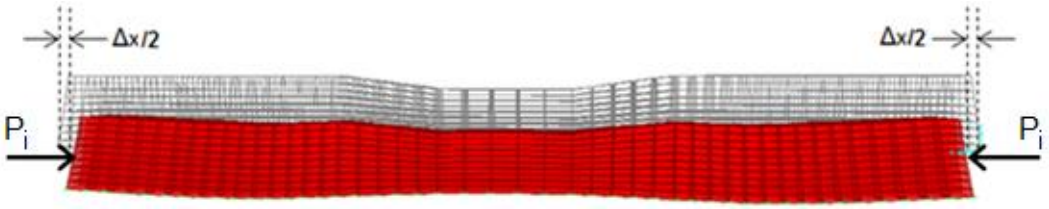

Fig. 11. Longitudinal prestressing force on the tie.

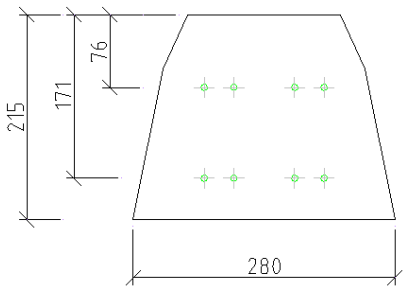

Fig. 12. Placement of prestressing wires within the ties.

Under service conditions, the joint action of the horizontal prestressing forces and vertical forces on the tie, induces bending around the lateral axis and compression along the longitudinal axis of the tie. Fig. 13 shows the resultant longitudinal compressive stresses due to bending and axial compression.

The joint action of 350 kN prestressing force and 270 kN vertical axle force induces longitudinal compressive stresses along the tie length varying up to 20 MPa. Fig. 13 shows that the 350 kN prestressing force diminishes the tensile longitudinal stresses.

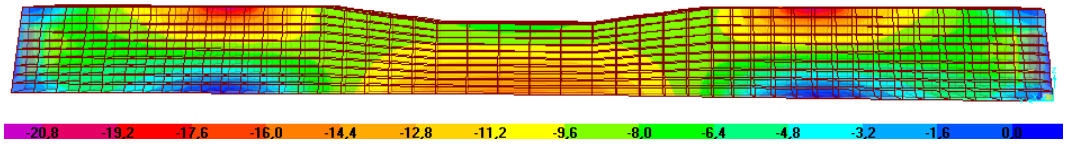

Fig. 13. Compressive stress distributions along tie due to axle and prestressing loads.

High strength prestressing strands with characteristic tensile strength f_{pk} = 1860 MPa with 0.1% proof stress of $f_{p0.1k}$ = 1290 MPa and 1% elongation stress of $f_{p1.0k}$ = 1440 MPa support the design prestressing force of P_i = 350 kN. The allowable tensile prestressing stress is the smaller of $0.9f_{p0.1k}$ = 1160 MPa or $0.8f_{p1.0k}$ = 1152 MPa. Eq. (3) shows the total prestressing area requirement.

$$A_{ts} = {P_i}/{0.8f_{p1.0k}} = 303 \text{ mm}^2 . \quad (3)$$

A steel strand with 7-mm diameter has an area of A_s = 38.4 mm². Eq. (4) shows the total number of strands needed to provide an initial prestressing force of P_i = 350 kN to the tie.

$$n = \frac{A_{ts}}{A_s} = \frac{303}{38.4} = 7.9 = 8 . \quad (4)$$

However, the introduced value of the initial prestressing into the tie does not remain constant but decrease in time due to elastic shortening of the tie with the prestressing, shrinkage and creep effects of concrete and the stress relaxation of the prestressing steel. Therefore, the designer must take into account the effective prestressing force that remains in the tie and gauge the occurrence of longitudinal tensile stresses in time. This particular design considered the performance of the tie under extreme dry conditions with a predicted prestress loss of 30% (Bezgin, 2015). The estimation of the prestress loss is the subject of another study.

7. Specification of Design Bending Moment Values for Ties under Service Conditions

The study presented up to this point summarizes the depth and extent of interactions of multiple parameters that are effective in the design of a railway tie under the action of service-level axle forces. The designer can reflect his or her understanding of the design requirements on the design of the tie in many ways with differing levels and depths of expertize. Understanding and estimation of the ballast support magnitudes and distributions, time dependent losses, axle forces and dynamic force estimations are dependent on the designer and different designs are possible for a given train speed and axle force.

However, a railway network consists of many individual routes. In today's world, transportation is a global matter extending beyond national borders. Therefore, differing designs between routes based on individual estimations of design parameters may generate railway lines with varying structural characteristics. These structural variations may limit service rate and service speed within or across networks and may generate difficulties in planning a track maintenance schedule. Such being the case, in order to provide a seamless integration of networks to the best extent possible, a cooperative approach among nations resulted with the formation of a Union of International Railways (UIC) with the aim of providing a common understanding of a design basis of railway tracks. Therefore, a unified methodology to determine tie design values is useful. The following subsections introduce the UIC-713R approach to estimate the tie design values for service level.

8. Service Load Design Values for the Ties

The design speed for the tie studies in this paper is 250 km/hour and its design static axle force is 225 kN. These values are typical in many countries in Europe, Turkey and the Middle East. Minimum ballast depth of the ballasted track is 350 mm and sub-ballast depth is 200 mm. Tie spacing with respect to their centers is 60 cm. Design track includes UIC-60 type rails with 60 kg/m mass and 172 mm depth. Tie service life is 40-years. The subsequent sections will present the dynamic axle loads and the related design moment values based on the UIC-713R suggestions.

8.1. Design axle force

Design moment values constitute the basis for tie design. The first set of design moment values are the ones that occur under ordinary service conditions. Service conditions relates to estimated rail support and track conditions. Eq. (5) relates the dynamic wheel load to static wheel load amplified by factors that reflect train speed and track conditions.

$$P_d = \frac{Q_0}{2}\left(1 + g_p . g_v\right) . g_d . g_r . g_i . \quad (5)$$

In the equation above, Q_0 = Static axle force, g_p = Impact attenuation factor by the bearing pad, g_v = Speed factor, g_d = Load distribution factor, g_r =Tie reaction variation factor due to support faults, g_i =Tie bottom irregularity factor. Impact attenuation factor relates to the characteristics of the elastomeric pads situated between the rails and the tie that reduce the impact of the rail onto the tie. Elasticity modulus of C60 grade high strength concrete used in this study is up to 6 times higher than the elasticity modulus of pinewood ties. Unlike the transition between a steel rail and wooden tie, the transition between a steel rail and high performance concrete tie is much stiffer due to higher stiffness of the concrete. Therefore, elastomeric pads reduce the magnitude of the

dynamic loads transferred from the steel rail to the concrete tie. Load distribution factor relates to the spacing of the ties and the attached rail bending rigidity and determines the percentage of the wheel force resisted by the tie underneath the wheel. Tie irregularity factor reflects possible production irregularities at the tie bottom that may amplify the applied loads.

The design values are: Q_0 = 225 kN, g_p = 1.0 for low attenuation, 0.89 for medium attenuation and 0.78 for high attenuation, g_v = 0.75, g_d = 0.5, g_r =1.35, g_i = 1.6. Eqs. (6) and (7) show the service level dynamic design wheel forces on ties supporting rails with medium impact attenuation and low impact attenuation elastomeric rail support pads, respectively.

$$P_{d-medium} = \frac{225}{2}\left(1 + 0.75 \cdot 0.89\right) \cdot 0.5 \cdot 1.35 \cdot 1.6 = 203 \text{ kN}, \quad (6)$$

$$P_{d-low} = \frac{225}{2}\left(1 + 0.75 \cdot 1.0\right) \cdot 0.5 \cdot 1.35 \cdot 1.6 = 213 \text{ kN}. \quad (7)$$

The dynamic estimate of the wheel force is 80% higher than the static wheel force for medium attenuated wheel forces and 90% higher for un-attenuated wheel forces. The particular design in this study included medium-attenuated bearing pad, the following section includes their force reducing effects.

8.2. Design moment values for service loads

Design dynamic service moment value relates to the dynamic wheel design forces determined in the previous section and the estimated support condition. Fig. 14 shows a proposed support condition that ignores the bearing pressure along the tie central region and considers the ballast bearing pressure underneath the rail seat uniformly distributing along to both sides of the rail seat. This reflects a reasonable consideration where most of the ballast support concentrates underneath the rail seats for a newly tamped track.

Fig. 15 shows half of the free body diagram of the rail seat region of the tie, hypothetically detached from its bearing pressure free central part. L_p is the distance between the rail seat central line and the tie end. Distance "e" considers the concrete confinement effect underneath the rail, thereby reducing the effective moment arm (L_e) with respect to the rail seat as, $L_e = L_p - e$. For a B70 type tie, L_p = 55 cm and for a UIC Type 60 rail bearing on the tie, e = 18 cm.

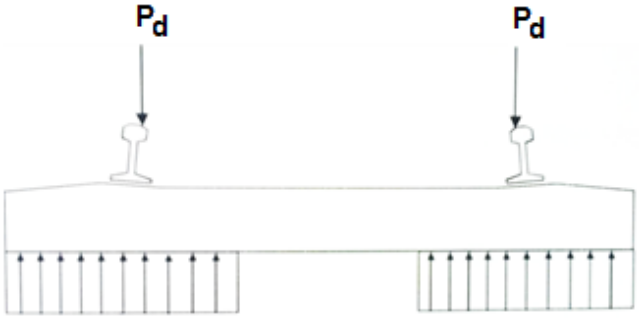

Fig. 14. Assumed ballast bearing pressure distribution underneath the tie (UIC-713R, 2004).

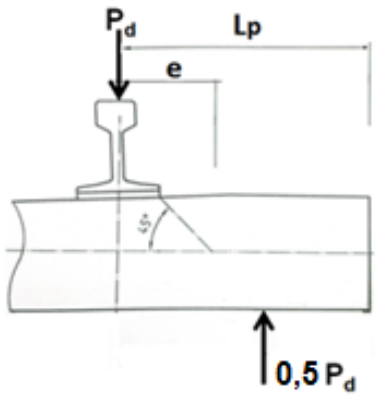

Fig. 15. Assumed ballast bearing pressure distribution underneath the tie (UIC-713R, 2004).

Eq. (8) relates the positive rail seat design bending moment under ordinary service conditions to the resultant ballast bearing force.

$$M_{dr}^{+} = P_d\left(\frac{L_p - e}{4}\right) = 203 \cdot \left(\frac{0.55 - 0.18}{4}\right) = 18.75 \text{ kNm}. \quad (8)$$

Based on the tie deformation shown in Fig. 3, the negative design bending moment at the tie center relates to the positive rail seat design bending moment and the ratio of the moment of inertia values of the tie central cross section and the rail seat cross section of the tie through Eq. (9).

$$M_{dc}^{-} \sim 1{,}2.M_{dr}^{+}\, {}^{I_c}/_{I_r}. \quad (9)$$

I_c and I_r are the moment of inertial values of the tie cross section at the tie center and at rail seats. Fig. 16 shows the longitudinal perspective of the 2600 mm long tie with its cross section dimensions at the rail seats and the middle of the tie.

The moment of inertia values of the tie at cross section A and B are I_r = 15,724 cm^4 and I_c = 8,465 cm^4 respectively. The ratio of the moment of respective moment of inertia values is 0.54 and the tie center negative design bending moment is determined in Eq. (10).

$$M_{dc}^{-} = 1.2 \cdot 18.75 \cdot 0.54 = 12.25 \text{ kNm}. \quad (10)$$

The positive sign for the moment at the rail seat signifies that the tie bottom at the rail seat is under tension. The negative sign for the moment at tie centre signifies that the tie bottom at the middle part of the tie is under compression.

An interesting finding through the estimated service values of maximum design bending moment service values is that the ratio of maximum design moments based on the UIC guidelines is $M_{dr}^{+}\text{max} / M_{dc}^{-}\text{max} \sim 1.53$, which is quite comparable to the ratio of maximum moments found earlier with the finite element analysis as $M_{r}^{+}\text{max} / M_{c}^{-}\text{max} \sim 1.38$. In other words, although UIC basis its tie design on a newly tamped track, it also accounts for the moment envelope bound by the possible variation of the ballast support stiffness and increased bending moments at the tie centre due to weakened ballast support.

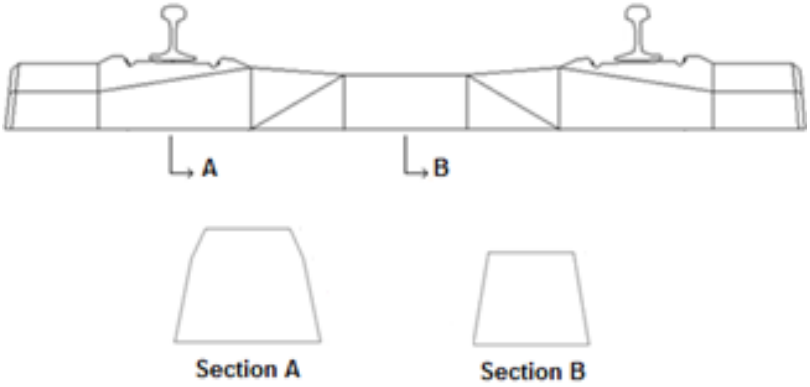

Fig. 16. Longitudinal profile and cross-section dimensions of the tie in mm.

One other useful finding is the comparison of the design service moment values found according to the UIC-713R with respect to findings based on an individually executed finite element analysis earlier and presented in Table 2. Unlike the UIC approach, the finite element approach in did not include the dynamic factor attenuation factor to account for the elastomeric bearing pads. In other words, the maximum design bending values included only the static value of the wheel forces. Therefore, in order to compare the results estimated by the two approaches, one must determine the static values of the M_{dr}^{+} and M_{dc}^{-} suggested by the UIC method.

Table 3 summarizes and compares the maximum static rail seat and tie centre design service moment values based on the two approaches. The static estimates of the two approaches for the rail seat and tie centre moment values are similar. The FEM estimates for the rail seat moment and the tie centre moments are respectively 85% and 95% of the UIC estimates. The lower aggrement for the rail seat moments is due to the fact that the finite element method approach considers a variable soil bearing pressure underneath the tie along rail seat whereas the UIC method assumes a constant bearing pressure at its maximum value.

Table 3. Comparison of static design service bending moment values of UIC and the FEM.

		UIC-713R estimates		FEM estimates		% ratio of FEM/UIC estimates
		Dynamic design moment (kN-m)	Load factor	Static design moment (kN-m)	Static design moment (kN-m)	
Tie rail seat moment	M_{dr}^{+}	18.75	1.90	9.87	8.44	85%
Tie centre moment	M_{dc}^{-}	12.25	1.90	6.45	6.11	95%
Moment ratio	M_{dr}^{+}/M_{dc}^{-}	1.53	-	1.53	1.38	90%

9. Conclusions

This paper presented an insight into the service load design of prestressed concrete high-speed railway ties. The first part presented the distribution of wheel loads to the ties and the variation of bending moments along a tie supported on ballast layers with different coefficient of subgrade reaction values. Determination of the required prestressing force for a tie under certain wheel loads and support conditions commenced. The study then compared the analytically estimated design moment values for the service load conditions to the values suggested by the UIC. The following list summarizes the numeric findings and recommendations resulting from this study.

- The maximum percentage of the wheel load transferred to a ties spaced at 60 cm center-to-center through a supporting a UIC-60 type rail is 48%, which confirms the existing recommendation of maximum wheel load transfer percentage of 50%.

- The sensitivity of the design moment value of the tie centre to ballast support conditions is higher than the rail seat due to a distinct variation of the ballast support bearing pressure distribution along the tie centre with varying coefficient of subgrade reaction.
- Tie centre moment linearly varies approximately by 0.22 kN-m and rail seat moment varies approximately by 0.03 kN-m per 0.05 N/mm^3 change in coefficient of subgrade reaction up to a value of 0.2 N/mm^3.
- The sensitivity of bending moment variations along the tie diminish above coefficient of subgrade reaction values above 0.2 N/mm^3.
- Bending analysis conducted on ties supported on ballast layers with coefficient of subgrade reaction values varying from C=0.02 MPa/mm and C=0.4 MPa/mm yielded ballast bearing pressure variations of 13% and 4% for the tie centre and tie rail seat respectively.
- The resultant bending moment variations for the tie centre and tie rail seat was 38% and 2% respectively.
- An overly stiff track bedding producing a coefficient of subgrade reaction beyond C=0.3 kN/mm^3 is unnecessary since the effect of higher C values on the generated moments diminish beyond this value.
- An overly stiff track bedding producing a coefficient of subgrade reaction beyond C=0.3 kN/mm^3 is unnecessary since the effect of higher C values on the generated moments diminish beyond this value.
- The ratio between maximum tie rail seat and tie centre moments based on the finite element analysis is approximately 1.38, which is close to and slightly less conservative than the UIC evaluation of 1.53.
- UIC design moment recommendations for the rail seat and tie centre is respectively 18% and 6% higher than the values obtained by the FEM, indicating estimations that are reasonably more conservative.

REFERENCES

American Railway Engineering and Maintenance of Way Association (2006). Manual for Railway Engineering. AREMA, Volume 1, Chapter 30, Part 1, "Ties – General Considerations".

Bezgin NÖ (2015). Climate effects on the shoulder width measurements of prestressed concrete high speed railway ties of ballasted tracks. *Measurement*, 75, 201–209.

Bezgin NÖ (2017). Development of a new and an explicit analytical equation that estimates the vertical impact loads of a moving train. *Procedia Engineering*, 189, 2-10.

Bezgin NÖ (2018). Proposal of a new analytical method to estimate the vertical impact forces on railway tracks due to changes in track profile and track stiffness. *CETRA 2018*, 837-843.

Ebrahimi A, Tinju MJ, Edil BT (2015). Deformational behavior of fouled railway ballast. *Canadian Geotechnical Journal*, 52(3), 344-355.

EN 13674 (2002). - Railway applications - Track - Rail - Part 1: Vignole railway rails 46 kg/m and above.

Indraratna B, Salim W, Rujikiatkamjorn C (2011). Advanced Rail Geotechnology – Ballasted Track. Taylor and Francis.

International Union of Railways (2004). Design of Monoblock Concrete Ties. UIC CODE, 713 R, 1st Edition.

Kerr A (2003). Fundamental of Railway Track Engineering. Simmons Boardman Pub Co, First Edition.

Kish A, Samavedam G (1991). Dynamic Buckling of Continuous Welded Rail Track: Theory, Tests, and Safety Concepts. Transportation Research Record 1289.

Lichtberger L (2005). Track Compendium: Formation, Permanent Way, Maintenance, Economics. Eurailpress.

Navikas D, Bulevičius M, Sivilevičius H (2016). Determination and evaluation of railway aggregate sub-ballast gradation and other properties variation. *Journal of Civil Engineering and Management*, 22(5), 699-710.